

# TECHNICAL NOTE

## D-1048

DETERMINATION OF LOCAL EXPERIMENTAL HEAT-TRANSFER  
COEFFICIENTS ON COMBUSTION SIDE OF AN  
AMMONIA-OXYGEN ROCKET

By Curt H. Liebert and Robert C. Ehlers

Lewis Research Center  
Cleveland, Ohio

NATIONAL AERONAUTICS AND SPACE ADMINISTRATION  
WASHINGTON

September 1961



## NATIONAL AERONAUTICS AND SPACE ADMINISTRATION

## TECHNICAL NOTE D-1048

DETERMINATION OF LOCAL EXPERIMENTAL HEAT-TRANSFER COEFFICIENTS  
ON COMBUSTION SIDE OF AN AMMONIA-OXYGEN ROCKET

By Curt H. Liebert and Robert C. Ehlers

## SUMMARY

Local experimental heat-transfer coefficients were measured in the chamber and throat of a 2400-pound-thrust ammonia-oxygen rocket engine with a nominal chamber pressure of 600 pounds per square inch absolute. Three injector configurations were used. The rocket engine was run over a range of oxidant-fuel ratio and chamber pressure. The injector that achieved the best performance also produced the highest rates of heat flux at design conditions. The heat-transfer data from the best-performing injector agreed well with the simplified equation developed by Bartz at the throat region. A large spread of data was observed for the chamber. This spread was attributed generally to the variations of combustion processes. The spread was least evident, however, with the best-performing injector.

## INTRODUCTION

The adequate cooling of the chambers and nozzles of chemical rocket engines requires design information for predicting the overall heat-transfer coefficient. The purpose of this investigation was to gain experimental gas-side heat-transfer data at various locations in a rocket engine and then determine whether any correlation scheme would predict the local gas-side heat-transfer coefficient. The literature suggests several analyses that may be applicable for predicting the heat transfer locally: That given by McAdams (ref. 1, p. 219), Bartz' simplified equation (ref. 2), Sibulkin's analyses (ref. 3), and flat-plate theory as given by Prandtl and Taylor, which may be adapted to fully developed flow in a tube (ref. 4, p. 207). The internal heat transfer and flow processes of the rocket engine are much more complex than the simplified models used in these references. Therefore, these analyses were evaluated as to their applicability in predicting the experimental data contained herein.

The uncooled rocket engine used was designed to produce 2400 pounds of thrust at a chamber pressure of 600 pounds per square inch absolute.

E-1133

CO-1

Liquid ammonia and oxygen were the propellants. These propellants gave clean combustion products, an important prerequisite for an experimental gas-side heat-transfer analysis. Three different injectors were used with this engine. A range of oxidant-to-fuel mass ratios with each injector and a limited number of low-chamber-pressure runs produced heat-transfer results over a range of Reynolds number and recovery temperature. The low-chamber-pressure runs were produced by reducing the total propellant flow rate. The chamber and nozzle geometry remained fixed.

The experimental gas-side heat-transfer coefficients were measured with a transient temperature technique. Instrumented thermal plugs were inserted in an uncooled, solid-wall rocket engine. The technique for inserting the thermal plug to physically approach one-dimensional heat-transfer conditions and the method for computing the heat-transfer coefficients from transient temperature measurements are discussed in reference 5. A discussion of the effect on the measured heat-transfer coefficient of a wall temperature discontinuity attributable to the thermal-plug installation and how this discontinuity affects the heat transfer results is contained herein.

The general heat-transfer results were analyzed with respect to the rocket-engine performance.

#### SYMBOLS

$c^*$	characteristic velocity
$c_p$	specific heat at constant pressure
$d$	diameter
$F$	fuel
$h$	surface coefficient of heat transfer
$Nu$	Nusselt number
$O$	oxidant
$O/F$	oxidant-to-fuel ratio
$Pr$	Prandtl number
$p_c$	chamber pressure
$Re$	Reynolds number

$r$  recovery factor  
 $r_c$  throat radius of curvature  
 $t$  temperature  
 $\rho$  density

Subscripts:

$a_l$  alumina-coated chamber  
 $Cu$  copper chamber  
 $ex$  experimental  
 $f$  film  
 $p$  plug  
 $r$  recovery  
 $s$  static  
 $t$  total  
 $th$  theoretical  
 $w$  wall

## APPARATUS

### Rocket Test Facility

The propellant flow system, thrust stand, rocket-engine ignition system, and instrumentation for rocket-engine performance are given in reference 6.

### Rocket Engine

The geometry of the solid-wall rocket engines used in this investigation is shown in figure 1. The thrust chambers were about 6 inches long. The inside diameter was approximately 3 inches, and the wall was 1 inch thick. Most of the tests were conducted with a steel chamber. In general, the inner wall of the chamber was covered with a 0.012-inch Nichrome base and a 0.010- to 0.015-inch aluminum oxide coating. Some tests were done with a copper chamber to evaluate the effects of wall temperature discontinuities on the heat-transfer measurements. Copper

nozzles consisting essentially of a throat section (2.03-in. diam.) and a short divergent section were used.

The thermal-plug installations in the chamber and throat are shown sectionally in figure 1. The function of the copper thermal plugs was to indicate the local transient heat transfer at the axial and circumferential positions indicated on the figure. An extensive description of these plugs and their instrumentation is presented in reference 5.

Three injector configurations were used. The injector elements were oriented with respect to the thermal-plug locations as shown in figure 2. A detailed description of hole sizes and injector pattern may be obtained from reference 6. The injector faces were made of nickel. Injector 1 consisted of 70 like-on-like impingement fuel holes, 66 like-on-like impingement oxidant holes, 4 showerhead fuel holes, and 27 showerhead oxidant holes. Injector 2 had 22 like-on-like impingement fuel holes and 22 showerhead oxidant holes. Injector 3 was made with 22 showerhead fuel holes and 22 like-on-like impingement oxidant holes. The fuel and oxidant holes in injector 1 were in general smaller than the holes in injectors 2 and 3. This achieved greater atomization for injector 1.

#### Instrumentation

The rocket-engine performance was measured by customary techniques. Propellant flow was measured with both turbine-type flowmeters and orifices and recorded. Thrust and chamber pressure were also recorded. Instrumentation was not provided to measure combustion instability. The important instrumentation associated with this facility was the thermometry and installation of the copper thermal plugs mounted in the walls of the engine.

Some revisions from the method described in reference 5 of the installation and placement of thermocouples on the copper plugs were made during the course of these experiments. It was found that heat loss from the cold end of the plug could be minimized by insulating the plug from the mild-steel cover that held the plug in place. This was accomplished by cutting a hole in the 0.250-inch-thick cover 0.005 inch deep and larger than the plug diameter. Thus, the cold end of the plug was insulated from the cover by an air gap. The plug was held in place by a screw through the top of the cover. The steel covers were welded to the steel chamber. The covers were bolted to the copper nozzle.

Chromel-Alumel thermocouples were located at the hot end, center, and cold end of the plug. The thermocouples were peened to the cold end of the plug and on the surface at the midportion of the plug. The hot-surface thermocouples were installed by drilling a hole along the axis of the plug and then peening the thermocouples in the bottom of the hole, which ended about 1/64 inch from the hot surface.

## PROCEDURE

### Experimental

The type of injector and the corresponding ranges of O/F, chamber pressure, and propellant flow achieved with each injector for obtaining the data under varying combustion conditions are indicated in table I. Table I shows that injector 1 was run at design conditions and also at off-design conditions at chamber pressures of 317, 344, and 350 pounds per square inch absolute. These lower chamber pressures were achieved by reducing the propellant flow.

Previous experience had shown that it was feasible to use injectors 1 and 3 only with steel, alumina-coated chambers. Injector 2 was run with an uncoated steel chamber. Two chambers, one copper and one steel with alumina coating, were run with injector 3 at O/F of 1.15 and 1.16 and chamber pressures of 572 and 585 pounds per square inch absolute, respectively, to observe the temperature-discontinuity effect across a thermal plug. (These data are shown in a later section.) The copper chamber did not fail during these tests because of the chamber wall's high heat-absorbing capacity.

### Reduction of Thermoplug Temperatures to Heat-Transfer Coefficients

The local transient rate of heat transfer and the local heat-transfer coefficients were calculated from the measured temperature distributions within the thermoplug element and the estimated steady-state gas-stream recovery temperature. The recovery temperature was estimated from

$$t_r = \left[ (t_t - t_s)r + t_s \right] \frac{c_{ex}^*}{c_{th}^*}$$

where  $r$  was taken as 0.9. Both the integration method and the constant  $h$  method discussed in reference 5 were used for reducing the transient-temperature data to heat-transfer coefficients.

The integration method is particularly applicable to these experiments because the burning times were short. The maximum duration of the burning times was 3 seconds, 0.8 second of which was needed to achieve steady combustion. The heat-transfer coefficients were obtained by plotting  $[pc_p t]_p$  against 3 thermocouple distances from the hot surface at burning times that differed by about 0.3 second. The time increment was taken after the start of steady combustion, thus eliminating the effect of the starting transient. The area between the curves was mechanically integrated to obtain the heat flux. Values of heat-transfer coefficient were calculated from the ratio of heat flux to the difference of recovery temperature and wall temperature averaged over the time increment considered.

When some thermocouples failed, as happened occasionally in these tests, it became necessary to incorporate the constant  $h$  method, which may be used to evaluate the heat-transfer coefficient  $h$ , with a minimum of one thermocouple. The constant  $h$  method makes use of the solution of the linear heat-flow equation in a dimensionless form. The graphical solutions presented in reference 7 were used to evaluate  $h$ . With this method it must be assumed that the combustion temperature, heat-transfer coefficient, and material properties are invariant with burning time. This method is good for cases where the burning time is long compared with the duration of the starting transient. The time increment needed in this solution was evaluated over the time of steady combustion.

E-1133

### Evaluation of Properties

Empirical equations formulated from nondimensional quantities such as Nusselt, Reynolds, and Prandtl numbers are often used to correlate heat-transfer results. Successful correlations have been achieved when the heat-transfer coefficient is based upon temperature and the thermodynamic and transport properties are evaluated at a film temperature,  $t_f = (t_s + t_w)/2$ . When recombination processes are present in the thermal boundary layer, the heat-transfer coefficient based on enthalpies and properties introduced at a reference enthalpy (ref. 4) is preferable to account for the recombination in the boundary layer. The properties at each point should be evaluated using the pressure, reference enthalpy, and gas composition at that point.

Calculations using several data points indicate negligible differences in the heat-transfer coefficient when based on temperatures or enthalpies for the range of conditions obtained herein. Also, the property values do not vary appreciably when evaluated at film or reference enthalpy conditions. Thus, temperatures were used to compute the heat-transfer coefficient, and properties were evaluated at film-temperature. The properties were obtained from reference 8 for combustion pressure of 600 pounds per square inch absolute and equilibrium composition for isentropic expansion.

### Accuracy of Results

The cumulative error attributable to the rocket performance in terms of  $c^*$  was estimated to be about 3 percent. This 3-percent error in performance is manifested as a 6-percent discrepancy in the estimation of the recovery temperature.

### Radiation Heat Transfer

No correction for radiation heat transfer was made for the data given in table I. Reference 8 indicates that water vapor will be the only product of combustion that will radiate to the wall. A calculation with water vapor for the conditions obtained herein indicates that in the rocket combustion chamber the radiation heat flux to the walls may be as high as 4 percent of the total energy transmitted to the wall. Radiation energy decreases throughout the nozzle to a negligible value at the throat.

### Transient-Technique-Solution Error

A comparison of the heat-transfer coefficients evaluated by both solution techniques when possible at the throat region showed that the constant  $h$  method differed from the integration method by about  $\pm 10$  percent.

### Wall-Temperature-Discontinuity Deviation

As indicated in reference 9, a step change in wall temperature disrupts the thermal boundary layer. Calculations based on the flat-plate theory of reference 9 indicate that steps of about  $500^{\circ}\text{F}$  greatly affect the local heat transfer. The introduction of a copper thermal plug in an alumina-coated steel wall produces such a step in the wall temperature. The effect of this temperature step on the measured heat flux was assessed experimentally. The heat-transfer data from copper plugs inserted in a copper chamber are compared with the data from copper plugs inserted in an alumina-coated steel chamber for comparable performance conditions and location in the following table:

	Plug A	Plug B	Circumferential variation, percent
$h_{\text{Cu}}$	0.00154	0.00175	13.6
$h_{\text{al}}$	0.00222	0.00254	14.4
Percent deviation in $h$ due to discontinuous surface temper- ature	44	45	

In addition to the 44- to 45-percent deviation due to the discontinuous surface temperature, there is one further significant result to be noted from this table. For both engine wall materials the percentage variations in the circumferential heat-transfer coefficient were almost identical. These limited tests seem to indicate that, even though temperature discontinuities are present, reliable data may be obtained on the percentage variation of circumferential heat flux. The total experimental error of  $h$  in the chamber may be quite large. The total error may accumulate to about 60 percent when the large temperature discontinuities, instrument errors, and transient-technique-solution errors are considered and radiation is neglected. Therefore, absolute values of  $h$  may be considered only qualitatively in the chamber.

Temperature measurements made in the copper chamber wall upstream of plugs A and B indicate temperature steps not greater than  $50^{\circ}$ . Therefore, it is reasonable to assume that the data at the throat are negligibly affected by temperature discontinuities because the copper plugs were mounted in a copper nozzle. The heat-transfer coefficient is also negligibly affected by radiation. Thus, the total experimental error in the heat-transfer coefficient at the throat is estimated to be about  $\pm 14$  percent.

## RESULTS AND DISCUSSION

### Rocket Performance

The  $c^*$  performance of the nominal 600-pound-per-square-inch-absolute-chamber-pressure, 2400-pound-thrust ammonia-oxygen rocket engine with three injector configurations is shown in table I. The data cover a range of oxidant-fuel ratios, and one injector was run at low chamber pressures. In discussing the data, the injectors will be referred to by the numbers designated in table I.

A comparison of  $(c_{ex}^*/c_{th}^*)$  values in table I indicates that injector 1, which incorporates the finer atomization and like-on-like elements for both propellants, gave the best performance. Injectors 2 and 3 exhibited about equivalent performance but at a level appreciably below that of injector 1. These results compare favorably with those of reference 6, which includes more performance data taken over a greater range of O/F.

### Heat Transfer

The experimental values of heat-transfer coefficient throughout the chamber and throat are tabulated in table I. The thermal-plug numbers in the table correspond to the letter-number designation in figure 1.

The reader should be reminded that the absolute values of the chamber data are greatly affected by the temperature discontinuity across the thermal plugs. The throat data are not appreciably affected by a temperature discontinuity. Because of the discrepancy in the chamber data, the throat and chamber data will generally be considered separately in the discussion of the heat-transfer data.

Chamber heat transfer. - As has been discussed in reference 10, heat transfer in the chamber may be unpredictable because of the complexity of the combustion process. Combustion in a rocket is composed of heterogeneous mixtures of burned and unburned propellants that produce local zones of gases of various mixtures. The local mixture ratios can be quite different from the measured overall mixture ratio entering the injector. The circumferential and longitudinal variations in heat-transfer coefficient given in table I indicate the nonuniformity of the combustion gases and perhaps the local scrubbing or eddying of these gases. The heat-transfer measurements achieved herein are a good means for evaluating an injector as to its capability for preparing propellants for a uniform energy release within the combustor.

From table I it is clear that the best-performing injector, injector 1 at high pressure, also produces the highest heat-transfer coefficient. These results may be attributed to the good atomization incorporated in injector 1.

While it is difficult to distinguish between the levels of performance of injectors 2 and 3 given in table I, it is apparent that the general level of heat transfer from injector 3 is greater than that of injector 2. This is especially obvious when the heat-transfer coefficients associated with these two injectors are compared at station III, the farthest downstream position of the plugs in the chamber. Table I indicates values of  $h$  at station III of about 0.000681 to 0.00146 Btu per second per square inch per  $^{\circ}\text{F}$  over the range of  $O/F$  considered with injector 2, while injector 3 shows values of  $h$  of about 0.00204 to 0.00355 Btu/(sec)(sq in.)( $^{\circ}\text{F}$ ). The design of injector 3 incorporates showerhead fuel holes that prepare the fuel poorly (ref. 6). Because of the poor fuel preparation, it is speculated that local combustion is occurring in the downstream end of the chamber, resulting in a different heat-transfer mechanism than turbulent pipe flow. The local combustion may produce eddying effects and appreciable changes in the thermal boundary layer. Later it will be observed that this downstream burning is probably affecting the nozzle heat transfer also. It can be concluded from this discussion that  $c^*$  is not always an accurate index of heat-transfer level; other factors such as local burning and local  $O/F$  must be considered.

Another important observation to be made from table I is that the percentage scatter in the heat-transfer data from all plugs is considerably less for the more efficient injector 1. The maximum percentage

E-1133

CO-2

scatter from a mean value over the O/F range considered is about  $\pm 26$  percent with injector 1 and  $\pm 100$  and  $\pm 46$  percent with injectors 2 and 3, respectively. This lends credence to the notion that a good injector produces a more uniform heat-flux distribution in the chamber.

Injector 1 was run at a low chamber pressure, and the results given in table I show an appreciable decrease in the heat transfer from the runs at design condition. This decay in heat transfer may be attributed to the inefficiency of the injector when run at an off-design condition and the lower propellant flows necessary during these tests when chamber pressure was lowered. These effects will be discussed in greater detail in the following sections.

Nozzle heat transfer. - As discussed previously, the throat data presented in table I represent reasonably correct values of the gas-side heat-transfer coefficient. It should be noted that at high chamber pressure the levels of these data follow the trends observed in the chamber; injector 1 shows the highest level, followed by injectors 3 and 2 in that order. The higher heat-transfer coefficients of injector 3 as compared with injector 2 are speculated to be due to the same downstream burning discussed in the preceding section on chamber heat transfer. The chamber data from injector 3 showed appreciably higher coefficients at the chamber exit in comparison to injector 2, which performed at about the same  $c^*$  level.

Off-design effect on nozzle heat transfer. - A comparison of the data in table I at high and low pressures with injector 1 indicates that the effect of operating the injector at off-design conditions on nozzle heat transfer is of about the same magnitude as observed in the chamber. This comparison further verifies the qualitative observations made with the chamber data. Heat-transfer correlations in nozzles indicate that the heat-transfer coefficient is almost directly proportional to pressure (ref. 11). However, the results of reference 11 were obtained from experiments that achieve lower chamber pressures with an injector operating at design conditions. The data obtained herein were achieved with an injector running at off-design conditions, and the heat-transfer coefficients given in table I are less than would be predicted from the results obtained in reference 11. Operating injector 1 at off-design conditions is probably causing incomplete combustion at the throat region, as evidenced by the lower performance. This may account for the disparity between the results of this experiment and the results of reference 11 obtained with an injector operating at design conditions.

Correlation of heat-transfer coefficients - An objective of this experimental program was to determine whether a correlation scheme would predict the local gas-side heat-transfer coefficient. Following the precedents of design practice and of the literature, the first approach used pipe-flow concepts. Any data to be correlated must correspond to complete combustion and full development of the thermal layer.

The heat-transfer data in the chamber for injectors 2 and 3 were considered not applicable to a pipe-flow correlation because of incomplete combustion. Because of the high efficiency of injector 1, it was thought that the heat-transfer measurements at the downstream station in the chamber would be compatible with the pipe-flow model. However, as was pointed out previously, these chamber data should be corrected for temperature step and radiation. The particular data were reduced 31 percent to approximate the wall temperature discontinuity and an additional 4 percent to correct for radiation heat transfer.

All the nozzle heat-transfer data (low and high pressure), in addition to the abovementioned chamber data, are plotted nondimensionally in figure 3. The fluid properties were evaluated at the film temperature. Because of the high efficiency of injector 1, the thermodynamic and transport data obtained from reference 8, which assumes 100-percent combustion efficiency, were considered pertinent to these data.

The data in figure 3 seem to fall into four groups: the corrected chamber data of injector 1 and three groups of data for nozzle throats, namely, the low-chamber-pressure data, the data from injector 2, and the data from injectors 1 (high pressure) and 3. The throat data of injector 2 and the low-pressure performance of injector 1 are at lower levels of  $Nu/Pr^{0.333}$ . The throat data of injector 3 and both the chamber and nozzle data of injector 1 are at higher levels of  $Nu/Pr^{0.333}$ .

It is difficult to explain why the throat data of injector 3 are greater than those of injector 2 because the  $c^*$  performance of each is comparable. Perhaps burning just upstream of the nozzle is affecting the nature of the throat thermal layer associated with injector 3. The possibility of this downstream burning was discussed previously.

Other than the exception (injector 3), the various levels of the throat data in figure 3 may be attributed to the  $c^*$  performance of the injectors.

The chamber and throat data of injector 1 are more likely to be comparable to values found in efficient rocket engines used in space applications. Weighting the throat data as the more reliable information, a suggested correlation for the data derived from injector 1 is:

$$Nu_f = 0.031 Re_f^{0.8} Pr_f^{0.333} \quad (1)$$

Unfortunately, there is an insufficient spread of Reynolds number in the throat data to verify the exponent on the Reynolds number. However, the 0.8 exponent has been verified in many heat-transfer studies of turbulent flow. Therefore, it is used herein. The arbitrarily corrected chamber data of injector 1 are about 35 percent above the prediction of equation (1).

From these limited data it does appear that the designer can use a pipe-flow correlation to estimate the heat-transfer coefficient in the throat region only. Equation (1) predicts the throat data of injector 1 operating at design conditions within a spread of  $\pm 6$  percent. Equation (1) also agrees well with steady-state data obtained at the throat of a rocket engine burning liquid ammonia and white fuming nitric acid at a chamber pressure of 500 pounds per square inch absolute (ref. 11). The good agreement of equation (1) with reference 11 indicates that the plug technique, when properly used, is a workable means for obtaining local heat-transfer data from uncooled, heavy-wall engines.

Comparison of results with analytical and correlated results in the literature. - Various correlations and analytical equations found in the literature were applied and compared with the data from injector 1. Film temperature was used to evaluate the properties in all cases. The relation suggested by reference 1, in the form  $Nu = 0.023Re^{0.8}Pr^{0.333}$ , predicts a coefficient that would be about 26 percent low compared with that of the equation through the best throat data (eq. (1)).

Bartz (ref. 2) gives a simple equation for rapid estimation of rocket-nozzle convective heat-transfer coefficients that may be expressed in the following way for comparison purposes:

$$Nu = 0.026Re^{0.8}Pr^{0.333}\left(\frac{d^1}{r_c}\right)^{0.1} \quad (2)$$

where  $d^1$  is throat diameter. The value of  $(d^1/r_c)^{0.1}$  for this application is 1.0302, thus reducing equation (2) to

$$Nu = 0.0268Re^{0.8}Pr^{0.333} \quad (3)$$

Thus, the Bartz equation would predict the data from injector 1 about 14 percent low.

An equation derived by Prandtl and Taylor for a flat plate, assuming turbulent temperature and velocity profiles with a laminar sublayer and adapted to fully developed flow in a tube in reference 4, predicts the heat transfer about 30 to 40 percent lower than the experimental results.

Several calculations based on Sibulkin's incompressible analysis (ref. 3) indicate that the analysis will predict the heat transfer between 38 and 61 percent higher than the experimental results. On the basis of these calculations for several data points, it is felt that the Sibulkin or Prandtl-Taylor analyses will not predict the experimental data accurately enough for engineering calculations. Bartz's equation and equation (1) predict the data accurately enough for most engineering

purposes. These limited experimental data should not be used to generalize on a method of correlation that includes rocket engines of different geometry and propellants from those used in these experiments. The conclusions stated herein apply only to one geometry and one propellant combination. These data should be of value to the designer because only a limited amount of local heat-transfer data are available from rocket firings.

### SUMMARY OF RESULTS

Heat-transfer coefficients have been experimentally determined in the chamber and throat of a nominal 2400-pound-thrust ammonia-oxygen rocket with a chamber pressure of 600 pounds per square inch absolute. The data were obtained over a range of chamber pressure and oxidant-fuel ratios with three injector configurations. For this propellant combination and rocket-engine geometry the following observations were made:

1. The equation  $Nu_F = 0.031 Re_F^{0.8} Pr_F^{0.333}$  predicted the throat heat-transfer data within a spread of  $\pm 6$  percent when a high-performing injector (injector 1) was operated at design conditions. Bartz's simple equation predicts the data about 14 percent lower than this equation.

2. Injector 1, which incorporated the best atomization, also gave the best performance and highest rates of heat transfer when operated at design conditions. The general level of heat-transfer from injector 3 was greater than that of injector 2. However, the performance of injectors 3 and 2 was about the same. Thus characteristic-velocity performance is not always a measure of the completeness of burning in the chamber or the amount of heat flux obtained at the throat. It is apparent that local heat transfer within rocket engines depends greatly on injector design.

3. The results in the chamber were considered only qualitatively, because the many complex phenomena associated with the combustion process make it virtually impossible to determine the heat-transfer effects explicitly. However, large circumferential and axial variations were noted, particularly with the lower performing injectors.

4. A large discontinuity in wall temperature due to the mounting of the plugs did not greatly affect observations of circumferential variations at a given axial position when the variations were made on a percentage basis. The absolute values of heat-transfer coefficient, however, were considerably affected.

Lewis Research Center

National Aeronautics and Space Administration

Cleveland, Ohio, June 7, 1961

## REFERENCES

1. McAdams, William H.: Heat Transmission. Third ed., McGraw-Hill Book Co., Inc., 1954.
2. Bartz, D. R.: A Simple Equation for Rapid Estimation of Rocket Nozzle Convective Heat Transfer Coefficients. Jet Prop. vol. 27, no. 1, Jan. 1957, pp. 49-51.
3. Sibulkin, Merwin: Heat Transfer to an Incompressible Turbulent Boundary Layer and Estimation of Heat-Transfer Coefficients at Supersonic Nozzle Throats. Jour. Aero. Sci., vol. 23, no. 2, Feb. 1956, pp. 162-172.
4. Eckert, E. R. G., and Drake, Robert M., Jr.: Heat and Mass Transfer. Second ed. McGraw-Hill Book Co., Inc., 1959.
5. Liebert, Curt H., Hatch, James E., and Grant, Ronald W.: Application of Various Techniques for Determining Local Heat-Transfer Coefficients in a Rocket Engine from Transient Experimental Data. NASA TN D-277, 1960.
6. Hendricks, Robert C., Ehlers, Robert C., and Graham, Robert W.: Evaluation of Injector Principles in a 2400-Pound-Thrust Rocket Engine Using Liquid Oxygen and Liquid Ammonia. NASA MEMO 12-11-58E, 1959.
7. Hatch, James E., Schacht, Ralph L., Albers, Lynn U., and Saper, Paul G.: Graphical Presentation of Difference Solutions for Transient Radial Heat Conduction in Hollow Cylinders with Heat Transfer at the Inner Radius and Finite Slabs with Heat Transfer at One Boundary. NASA TR R-56, 1960.
8. Gordon, Sanford, and Glueck, Alan R.: Theoretical Performance of Liquid Ammonia with Liquid Oxygen as a Rocket Propellant. NACA RM E58A21, 1958.
9. Hartnett, J. P., Eckert, E. R. G., Birkebak, Roland, and Sampson, R. L.: Simplified Procedures for the Calculation of Heat Transfer to Surfaces with Non-Uniform Temperatures. TR 56-373, WADC, Dec. 1956.
10. Bartz, Donald R.: The Role of Transport Properties in the Problems of Jet Engines and Rockets. EP 405, Jep Prop. Lab., C.I.T., Aug. 1, 1957.

11. Rose, Robert Koeberle: Experimental Determination of the Heat Flux Distribution in a Rocket Nozzle. Rep. F-58-1, Purdue Univ. Rocket Lab., Jan. 1958.

TABLE I. - PERFORMANCE AND HEAT-TRANSFER DATA

Oxidant-fuel ratio, O/F	Chamber pressure, $p_c$ , lb/sq in. abs	Propellant flow, lb/sec	$c_{ex}^*$	$\frac{c_{ex}^*}{c_{th}^*}$	Plug location and number	<sup>a</sup> Heat-transfer coeff., $h$ , Btu/(sec)(sq in.)(°F)	Copper-plug wall temp., $T_F$ (for correlation purposes)
Injector 1: Atomization, F and O fine Impingement							
1.228	554	10.62	5440	0.936	C-1	0.00745	1529
					C-2	.00575	1236
					C-3	.00467	998
					C-4	.00656	1514
					C-5	.00504	1484
					C-7	.00514	1385
					T-1	{.00462}	1555
					T-3	{.00456}	1682
1.500	573	10.42	5686	0.992	T-1	{0.00525}	1390
					T-2	{.00555}	1340
1.670	564	10.71	5448	0.976	T-1	{0.00477}	1317
					T-2	{.00486}	1610
1.733	568	10.76	5459	0.986	C-1	0.00766	1700
					C-2	.00574	1340
					C-3	.00720	1700
					C-4	.00736	1720
					C-5	.00604	1560
					C-6	.00482	1258
					C-7	.00495	1550
					T-1	{.00478}	1375
					T-2	{.00471}	1502
					T-3	{.00464}	1308
1.222	317	6.413	5158	0.888	C-1	0.00153	540
					C-2	.00115	354
					C-3	.00100	277
					C-4	.00204	644
					C-5	.00189	618
					C-7	.00150	665
					T-1	{.00207}	534
					T-3	{.00176}	467
1.442	344	7.014	5111	0.885	C-1	0.00163	610
					C-2	.00108	373
					C-3	.000899	292
					C-4	.00186	698
					C-5	.00181	656
					C-7	.00146	719
					T-1	{.00201}	666
					T-3	{.00169}	607
1.507	350	7.231	5047	0.882	C-1	0.00180	604
					C-2	.00114	375
					C-3	.000899	288
					C-4	.00192	662
					C-5	.00163	612
					C-7	.00180	702
					T-1	{.00194}	676
					T-3	{.00192}	658

<sup>a</sup>The total experimental error in the heat-transfer coefficients shown in braces is estimated to be about  $\pm 14\%$ . The coefficients not braced are affected by the discontinuity error as discussed in the text and may be high by 60%.

TABLE I. - Concluded. PERFORMANCE AND HEAT-TRANSFER DATA

Oxidant-fuel ratio, O/F	Chamber pressure, $p_c$ , lb/sq in. abs	Propellant flow, lb/sec	$c_{ex}^*$	$\frac{c_{ex}^*}{c_{th}^*}$	Plug location and number	$h$ , Btu/(sec)(sq in.)(°F)	Copper-plug wall temp., °F (for correlation purposes)
Injector 2: Atomization, F coarse impingement, O showerhead							
1.47	578	11.67	5171	0.899	C-1	0.000322	332
					C-2	.000477	300
					C-3	.000660	332
					C-4	.000681	460
					C-5	.00111	612
					C-7	.00132	691
					T-1	{.00326}	953
					T-2	{.00296}	925
					T-3	{.00309}	965
1.748	553	11.47	5038	0.913	C-1	0.000306	258
					C-2	.000413	280
					C-3	.000592	295
					C-4	.000650	435
					C-5	.000927	519
					C-7	.00146	736
					T-1	{.00278}	1100
					T-2	{.00269}	1110
					T-3	{.00262}	1077
1.922	569	11.79	5004	0.929	C-1	0.000236	186
					C-2	.000370	255
					C-3	.000393	247
					C-4	.000324	290
					C-5	.000681	511
					C-7	.000850	523
					T-1	{.00251}	1190
					T-2	{.00257}	1230
					2.060	566	11.91
C-2	.000428	231					
C-3	.000409	252					
C-4	.000401	238					
C-5	.000792	355					
C-7	.000836	449					
T-1	{.00245}	962					
T-2	{.00257}	1050					
Injector 3: Atomization, O coarse impingement, F showerhead							
1.046	518	10.57	5105	0.899	C-6	0.00233	872
					C-7	.00204	807
					T-1	{.00402}	1343
					T-2	{.00430}	1480
					T-3	{.00360}	1340
1.295	561	10.94	5345	0.9175	C-1	0.00189	763
					C-2	.000737	415
					C-3	.00101	550
					C-4	.00282	1200
					C-5	.00287	1150
					C-6	.00329	1400
					T-2	{.00433}	1460
					T-3	{.00409}	1471
					1.445	530	10.65
C-2	.000930	510					
C-3	.00127	602					
C-4	.00323	1283					
C-5	.00345	1310					
C-6	.00355	1462					
T-2	{.00425}	1546					
T-3	{.00396}	1496					

<sup>a</sup>The total experimental error in the heat-transfer coefficients shown in braces is estimated to be about  $\pm 14\%$ . The coefficients not braced are affected by the discontinuity error as discussed in the text and may be high by 60%.

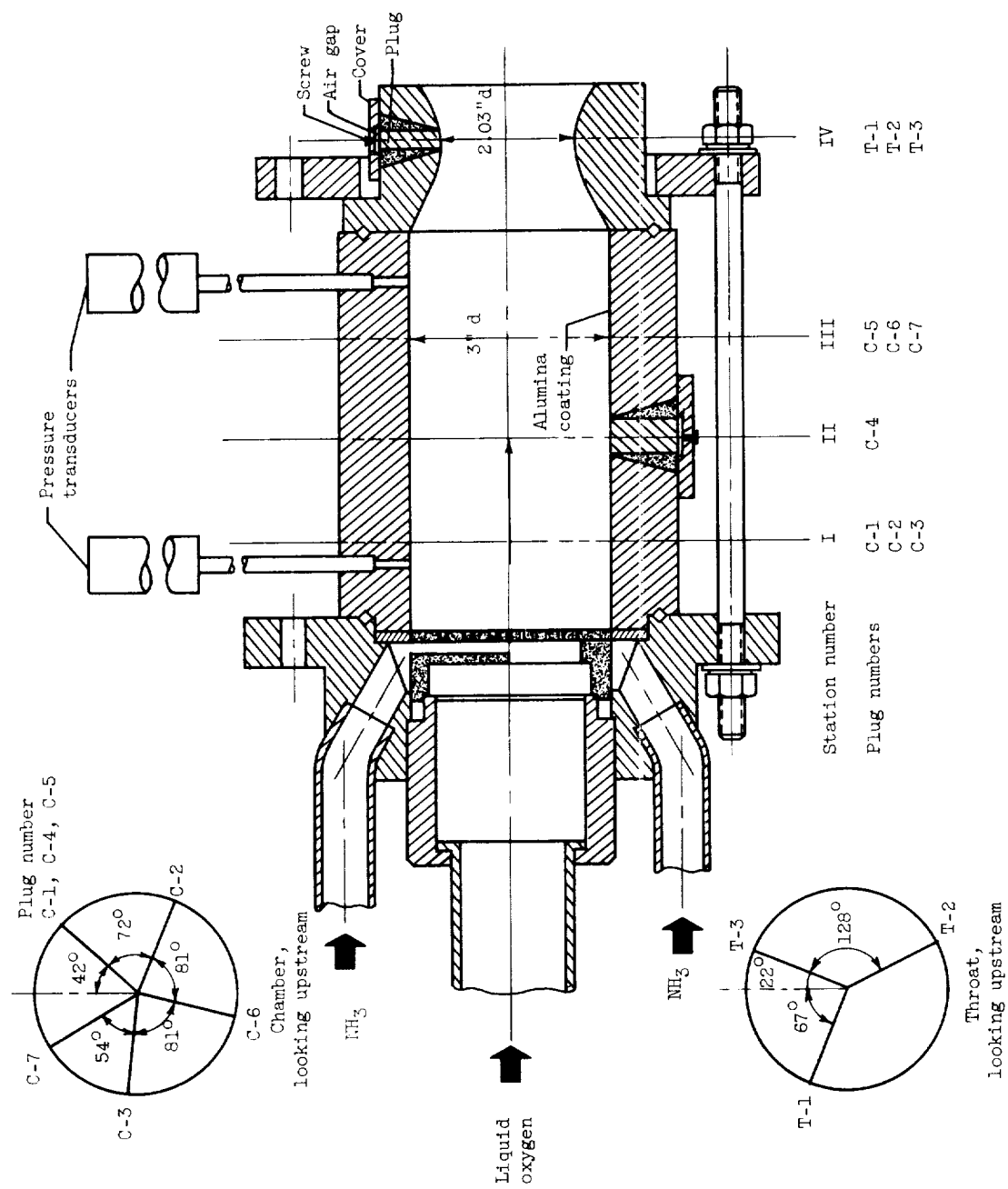


Figure 1. - Assembly of rocket motor and installation of copper plugs in rocket wall.

E-1133

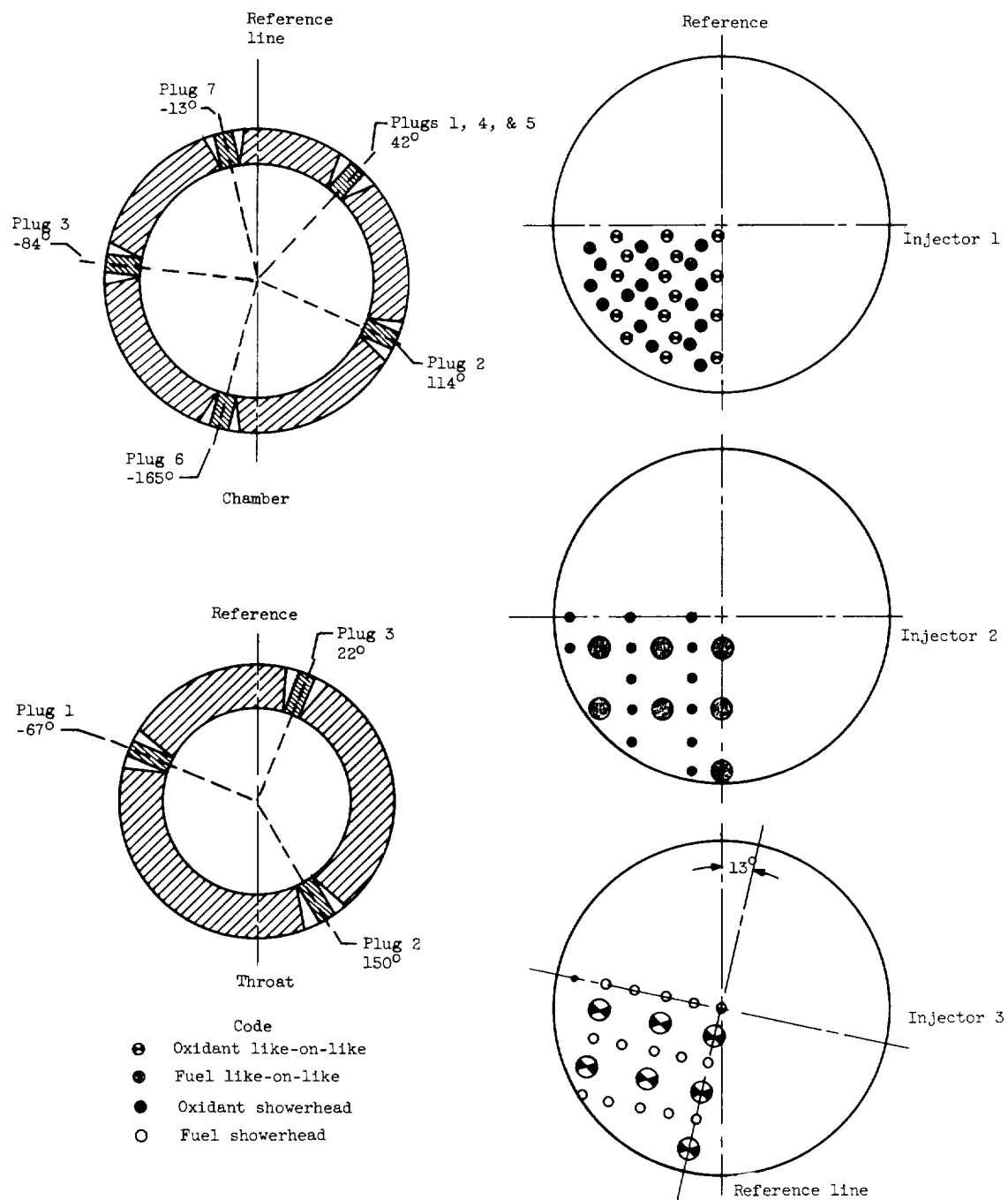


Figure 2. - Orientation of plug distribution in chamber and throat to injector face looking upstream.

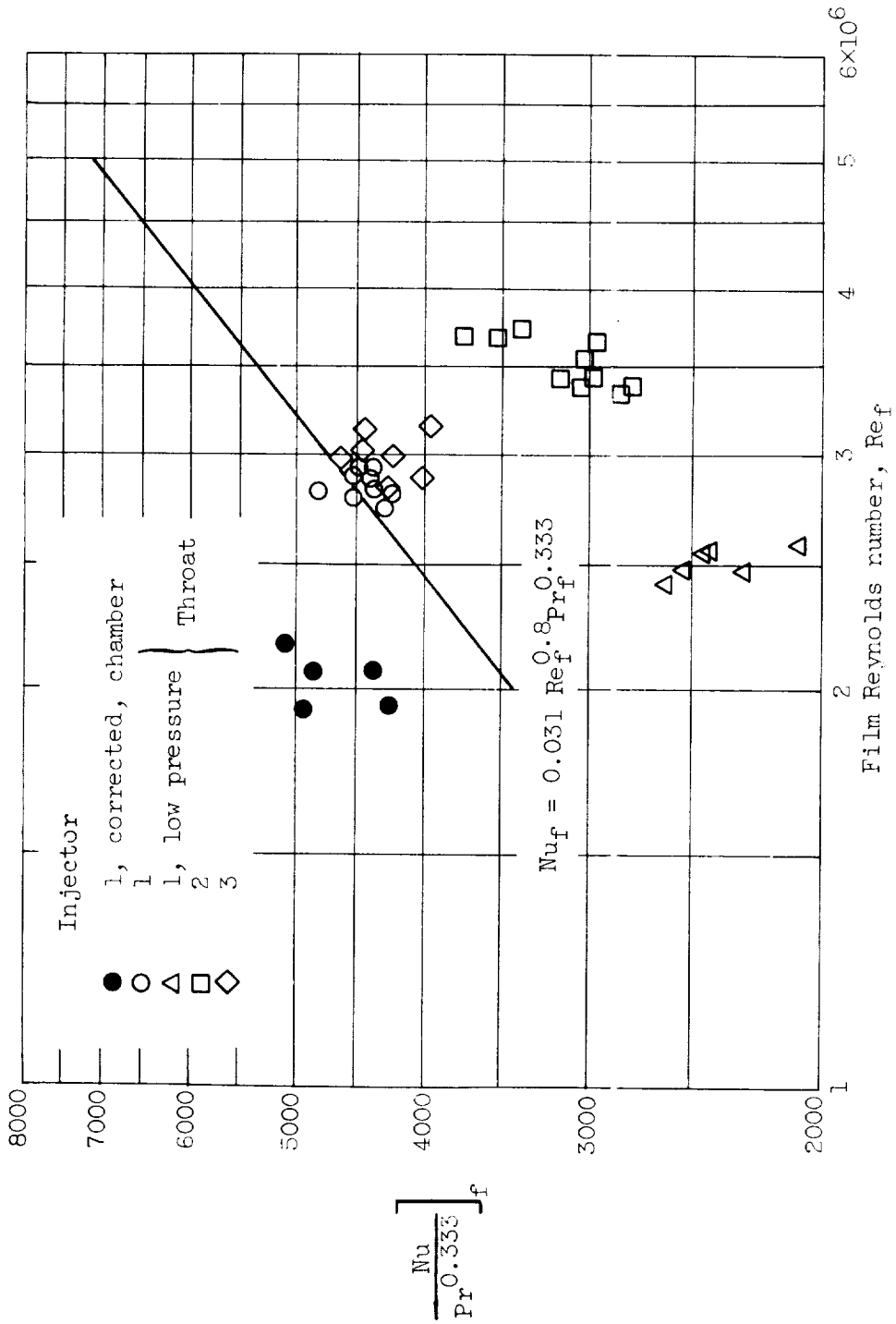


Figure 3. - Experimental heat-transfer coefficients at nozzle throat.